excited $^5T_1$ for $Co(H_2O)_6^{3+}$ should therefore be close to the $^1A_1$ ground state in energy. The analysis of Winkler et al.[31] as well as much earlier considerations by Friedman et al.[32] suggest that the energy difference is only about 4 kcal mol^{-1} with a rather much larger equilibrium distance for the $^5T_1$ state. The latter result is in agreement with spectroscopic results[19] as well as our calculations for $Co(NH_3)_6^{3+}$. Thus the $^5T_1$ state has an equilibrium bond length that is much closer to the one for the ground state of the Co(II) complex. This suggests a possible electron-transfer path via the $^5T_1$ or $^3T_1$ state for $Co(H_2O)_6^{2+/3+}$.[33] In the case of $Co(NH_3)_6^{3+}$ the $^5T_1$ is too high in energy,[19] however, to be of any importance as a preequilibrium state for electron transfer.

VI. Conclusions

Electron exchange between $Co(NH_3)_6^{2+}$ and $Co(NH_3)_6^{3+}$ in their respective ground states is spin forbidden in the absence of spin-orbit coupling. We suggest that the ^2E state for $Co(NH_3)_6^{2+}$ is closer in energy to the ground state ($^4T_1$) than believed previously. This suggestion is supported by INDO calcuations. In fact for small metal-ligand distances there is a crossing between the ^2E and $^4T_1$ energy surfaces. Thus for Co-N distances appropriate for electron transfer, the ^2E state is below the $^4T_1$ state. Due to spin-orbit coupling the $^4T_1$ states pass adiabatically to the ^2E state. Electron exchange between the ^2E state of $Co(NH_3)_6^{2+}$ and the $^1A_1$ state of $Co(NH_3)_6^{3+}$ is spin-allowed. The attempt was made to estimate whether the electron transfer between the two complexes, held close to each other in various conformations, was also spatially adiabatic. As for $Fe(H_2O)_6^{2+/3+}$, we found that $Co(NH_3)_6^{2+/3+}$ was close to the border to nonadiabatic electron transfer.

The ^2E intermediate state, according to our calculations with all Co-N distances equal, lowers the thermal barrier for electron transfer somewhat. Since Jahn-Teller distortion of the ^2E state takes place, the barrier is again increased. Our calculations suggest, however, that the ^2E barrier is still lower than or is about the same as the $^4T_1$ barrier. This is in agreement with experimental results.[3,4]

Acknowledgment. We are grateful for continued support from NFR, the Swedish Natural Science Research Council (S.L., K.S.), and from the United States Army through CRDC Chemical Systems Technology Center Award DAAA 15-85-C-0034 (M.C.Z.).

Registry No. $Co(NH_3)_6^{2+}$, 15365-75-0; $Co(NH_3)_6^{3+}$, 14695-95-5.

Contribution from the Department of Chemistry, Boston University, Boston, Massachusetts 02215, and National Bureau of Standards, Gaithersburg, Maryland 20899

Mechanisms of Ligand-to-Metal Intramolecular Electron Transfer in Cobalt(III)-Amine Complexes Containing a Coordinated Radical[1]

Kevin D. Whitburn,[†] Morton Z. Hoffman,*[‡] Nina V. Brezniak,[‡] and Michael G. Simic[§]

Received January 15, 1986

The one-electron reduction of Co(III) complexes containing nitrophenyl ligands possessing differing lead-in and bridging groups by radiolytically generated $^{\bullet}CO_2^-$ and $^{\bullet}C(CH_3)_2OH$ radicals in neutral and acidic aqueous solution results in the formation of coordinated nitrophenyl ligand radicals. The UV-visible absorption spectra, the acid-base properties, and the decay kinetics of the transient intermediates were examined by pulse radiolysis. In neutral solution, the coordinated ligand radicals decay via intramolecular electron transfer from the coordinated nitrophenyl radical donor to the Co(III) acceptor. The values of the intramolecular electron-transfer rate constants depend on the isomeric position of the nitro group on the phenyl moiety, the structure of the bridging molecule between the redox sites, and the nature of the lead-in group to the metal center. Bridging structures between the initial radical site and the metal center of varying length, flexibility, and π-conjugation are incorporated into the 18 complexes studied. Correlation of the values of $\Delta H^{\ddagger}$ and $\Delta S^{\ddagger}$ of electron transfer with the structural relationship of the donor and acceptor sites leads to the proposition that four different mechanisms of intramolecular electron transfer operate in these complexes: through chain, direct and indirect ligand bypass, and nonadiabatic transfer. Protonation of the coordinated nitro radical greatly diminishes the rate of intramolecular electron transfer in the nitrophenyl carboxylato complexes; in most cases, protonation affects only the driving force for electron transfer while leaving the mechanism unchanged.

Introduction

The study of the rates and mechanisms of electron-transfer reactions is fundamental to the understanding of many important biological redox sequences, including the respiratory chain and photosynthesis.[2] At the basis of these biological processes is the controlled sequential transfer of electrons between protein molecules that contain specific redox-active sites. Beyond its biological relevance, the understanding of the mechanisms of electron transfer between separated donor and acceptor sites has application to redox processes on electrode surfaces and to the reactivity of intermediates in homogeneous and heterogeneous catalysis. When the donor and acceptor sites are on a single molecule, electron transfer can occur intramolecularly without the kinetic influences of reactant diffusion and precursor substitution. These intramolecular systems, based conceptually on early developments by Taube,[3] model the "precursor complex" that precedes electron transfer in bimolecular redox reactions.[4]

The relationship between the rate of intramolecular electron transfer (IET) and the distance between the donor and acceptor sites has been examined by a number of investigators with a particular focus on long-range reactivity.[5-13] The relationship

[†] Present address: Department of Chemistry, Framingham State College, Framingham, MA 01701.
[‡] Boston University.
[§] National Bureau of Standards.

(1) This research was supported by a grant from the Office of Basic Energy Sciences, Division of Chemical Sciences, U.S. Department of Energy, to Boston University.
(2) Isied, S. S. *Prog. Inorg. Chem.* **1984**, *32*, 443.
(3) Isied, S. S.; Taube, H. *J. Am. Chem. Soc.* **1973**, *95*, 8198.
(4) Sutin, N. *Acc. Chem. Res.* **1968**, *1*, 225.
(5) Winkler, J. R.; Nocera, D. G.; Yocom, K. M.; Bordignon, E.; Gray, H. B. *J. Am. Chem. Soc.* **1982**, *104*, 5798.
(6) Kostic, N. M.; Margalit, R.; Che, C.-M.; Gray, H. B. *J. Am. Chem. Soc.* **1983**, *105*, 7765.
(7) Nocera, D. G.; Winkler, J. R.; Yocom, K. M.; Bordignon, E.; Gray, H. B. *J. Am. Chem. Soc.* **1984**, *106*, 5145.
(8) Isied, S. S.; Worosila, G.; Atherton, S. J. *J. Am. Chem. Soc.* **1982**, *104*, 7659.
(9) Isied, S. S.; Kuehn, C.; Worosila, G. *J. Am. Chem. Soc.* **1984**, *106*, 1722.
(10) Peterson-Kennedy, S. E.; McGourty, J. L.; Hoffman, B. M. *J. Am. Chem. Soc.* **1984**, *106*, 5010.
(11) Ho, P. S.; Sutoris, C.; Liang, N.; Margiolash, E.; Hoffman, B. M. *J. Am. Chem. Soc.* **1985**, *107*, 1070.
(12) Calcaterra, L. T.; Closs, G. L.; Miller, J. R. *J. Am. Chem. Soc.* **1983**, *105*, 670.
(13) Miller, J. R.; Calcaterra, L. T.; Closs, G. L. *J. Am. Chem. Soc.* **1984**, *106*, 3047.

0020-1669/86/1325-3037$01.50/0

between the mechanism of electron transfer and the structure of the molecular medium between the redox-active sites has also been studied systematically. The role of the bridging chain has been investigated for IET across polypeptides in which flexible and rigid amino acid residues have been positioned between the donor and acceptor metal ions in a series of binuclear complexes.[14] Binuclear complexes in which the donor and acceptor metal ions are separated by organic bridging molecules having variable flexibility and extent of π-conjugation have been systematically studied.[15] Depending on the precise nature of the bridging ligand, either through-the-bridge or bridge-bypass mechanisms are operative.

Another experimental approach to the study of IET in metal complexes involves the generation of a nitrophenyl donor radical at a remote ligand site of a pentaamminecobalt(III) complex.[16] The rate of IET, investigated as a function of the isomeric position of the nitro group in a series of mono- and dinitrobenzoato complexes, depends on the electron spin density at or adjacent to the carboxyl group leading into the Co(III) acceptor center.[17,18] The generally slow rate of IET in these Co(III) complexes relative to molecular vibration has been attributed to the poor overlap of the π-orbitals of the ligand with the σ-orbitals of the Co(III) center.[17,19] The insulating effect of the carboxyl lead-in group may reinforce inherent structural tendencies for transferring an electron from the ligand radical directly into the metal center in an "intramolecular outer-sphere" mechanism that bypasses the lead-in group.[19,20]

In this paper we report the rates of IET studied as a function of solution medium for 18 Co(III) complexes containing nitrophenyl ligands that possess organic bridging structures of variable length, flexibility, π-conjugation, and isomeric disposition of the nitro group on the aromatic portion of the remote ligand and variable lead-in groups to the acceptor center. From the observed activation parameters, four mechanisms of IET are proposed to be operative in these complexes. A preliminary account of some of these results has been published previously.[21]

Experimental Section

Preparation of Complexes. General literature methods were used to prepare (nitrophenyl carboxylato)pentaamminecobalt(III) complexes as the perchlorate salts.[22,23] The parent nitrophenyl acids used in the syntheses were purchased from Aldrich and ICN Biochemicals. Any parent acids received that were off-white were recrystallized from boiling methanol. Analyses of melting points before and after recrystallization were taken as general indicators of the purity of these starting materials. Crude samples of the complexes were, in general, not purified of unreacted acid by the literature method of repeated washings with methanol and ether, because several of the complexes were soluble in these organic solvents. Instead, the unreacted acid was removed by dissolving the crude sample in a minimum amount of water at 70 °C to which a saturated $NaHCO_3$ solution was added dropwise until the pH was ~9. The solution was then quickly chilled to 0 °C with stirring on a salt–ice bath to minimize any base hydrolysis of the precipitating complex; any reacted acid remained in solution as its sodium salt. The filtered complex was then recrystallized two to three times from water at 70 °C and dried in a desiccator. Elemental analyses for Co, N, C, and H were satisfactory, indicating the presence of, at most, negligible quantities of the free ligand parent acids. UV–visible spectra were taken of the nitrophenyl carboxylato complexes; characteristic d–d bands having absorbance maxima at 500–502 nm with $\epsilon \sim 10^2$ M^{-1} cm^{-1} were observed.

Other complexes were kindly provided by other researchers: ((*p*-nitrophenyl)cyano)pentaamminecobalt(III) perchlorate and (3-((*p*-nitrophenyl)carbonyl)-2,4-dimethyl-1,5,8,12-tetraazacyclotetradeca-1,3-diene)cobalt(III) hexafluorophosphate (Dr. R. J. Balahura, University of Guelph); (((*p*-nitrophenyl)amino)sulfonyl)pentaamminecobalt(III) perchlorate and (*p*-nitrophenoxo)pentaamminecobalt(III) perchlorate[24] (Dr. R. B. Jordan, University of Alberta); ((*p*-nitrophenyl)sulfonyl)-pentaamminecobalt(III) perchlorate (Dr. W. G. Jackson, Australian National University). The reduced Co(II) form of the macrocyclic complex was characterized spectrally by reduction with V(II) solution.[25]

Table I. Co(III) Complexes Studied[a]

ligand	X	Y	abbrev
o-nitrobenzoate		O_2C	ONBZ
m-nitrobenzoate		O_2C	MNBZ
p-nitrobenzoate		O_2C	PNBZ
(*o*-nitrophenyl)acetate	CH_2	O_2C	ONPA
(*m*-nitrophenyl)acetate	CH_2	O_2C	MNPA
(*p*-nitrophenyl)acetate	CH_2	O_2C	PNPA
(2,4-dinitrophenyl)acetate	CH_2	O_2C	DNPA
o-nitrocinnamate	CH=CH	O_2C	ONCM
m-nitrocinnamate	CH=CH	O_2C	MNCM
p-nitrocinnamate	CH=CH	O_2C	PNCM
(*p*-nitrophenyl)butyrate	$(CH_2)_3$	O_2C	PNPB
(*p*-nitroglycyl)benzoate	$CONHCH_2$	O_2C	PNGB
(*p*-nitrophenyl)diglycinate	$(CONHCH_2)_2$	O_2C	PNDG
(*p*-nitrophenyl)cyanide		NC	PNNC
((*p*-nitrophenyl)amino)sulfonyl		$NHSO_2$	PNNS
(*p*-nitrophenyl)sulfonyl		OSO_2	PNOS
p-nitrophenoxide		O	PNPO
nitrotetraazamacrocycle[b]			NCYC

[a] $(NH_3)_5Co$–Y–X–$PhNO_2$: X = bridging group; Y = lead-in group. [b] Macrocycle structure:

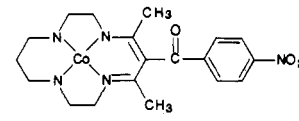

The complexes used in this study are of the form Co^{III}–Y–X–$PhNO_2$ (where X is the bridging group and Y is the lead-in group) and are shown in Table I.

Radiation Techniques. Pulse radiolyses were conducted with the Febetron 705 apparatus at the U.S. Army Natick Research and Development Center or the van de Graaff accelerator at the Center for Fast Kinetics Research (CFKR) at the University of Texas, Austin. Transient absorption spectra were obtained by optical spectrophotometry with time resolutions of <0.5 μs. The radiation dose per pulse was determined from SCN^- dosimetry.[26] Experiments were normally run at 25 °C; activation parameters were obtained with temperature control to ±0.2 °C. Continuous radiolyses were performed with the ^{60}Co γ-source at Boston University. Fricke dosimetry[27] was used to evaluate the dose rate (D_r) of the γ-source, for which a value of 1.1×10^2 Gy min^{-1} was determined.

Solutions to be irradiated were prepared in water purified through Millipore systems. Reagent grade sodium formate (Fisher) and 2-propanol (Eastman) were used, and solutions were buffered with sodium phosphate and adjusted to the desired acidic pH with perchloric acid. Solutions were purged of air by bubbling for ~30 min with high-purity N_2O. Analyses for Co_{aq}^{2+} after γ-irradiation were performed by using the method of Kitson[28] with a Cary 118 spectrophotometer. Yields of Co_{aq}^{2+} were linear with radiation dose. The extent of radical-induced reaction was kept to <15%.

Generation of Reducing Radicals. Reaction 1 represents the stoichiometry of the radiolysis of water and dilute aqueous solutions; the G values, or molecular yields of the primary species per 100 eV of energy, are shown in parentheses. In N_2O-saturated solutions, e_{aq}^- is rapidly

$$H_2O \rightarrow e_{aq}^- (2.8), {}^{\bullet}OH (2.8), H^{\bullet} (0.6), H_2O_2 (0.7) \qquad (1)$$

converted to $^{\bullet}OH$; in acidic solutions, e_{aq}^- is rapidly converted to $^{\bullet}H$. In the presence of formate or 2-propanol, the $^{\bullet}OH$ and $H^{\bullet}$ radicals react by H-abstraction to generate the secondary reducing radicals $^{\bullet}CO_2^-$ and $^{\bullet}C(CH_3)_2OH$, respectively.[17] The relative concentrations of a given Co(III) complex and the organic solutes were chosen so that >95% of

(14) (a) Isied, S. S.; Vassilian, A. *J. Am. Chem. Soc.* **1984**, *106*, 1726; (b) Isied, S. S.; Vassilian, A. *J. Am. Chem. Soc.* **1984**, *106*, 1732.
(15) Haim, A. *Pure Appl. Chem.* **1983**, *55*, 89.
(16) Hoffman, M. Z.; Simic, M. *J. Am. Chem. Soc.* **1972**, *94*, 1757.
(17) Simic, M. G.; Hoffman, M. Z.; Brezniak, N. V. *J. Am. Chem. Soc.* **1977**, *99*, 2166.
(18) Neta, P.; Simic, M. G.; Hoffman, M. Z. *J. Phys. Chem.* **1976**, *80*, 2018.
(19) Wieghardt, K.; Cohen, H.; Meyerstein, D. *Ber. Bunsen-Ges. Phys. Chem.* **1978**, *82*, 388.
(20) Hoffman, M. Z.; Simic, M. *J. Am. Chem. Soc.* **1970**, *92*, 5533.
(21) Whitburn, K. D.; Hoffman, M. Z.; Simic, M. G.; Brezniak, N. V. *Inorg. Chem.* **1980**, *19*, 3180.
(22) Gould, E. S.; Taube, H. *J. Am. Chem. Soc.* **1964**, *86*, 1319.
(23) Dockal, E. R.; Everhart, E. T.; Gould, E. S. *J. Am. Chem. Soc.* **1971**, *93*, 5561.
(24) Solutions of the PNPO complex undergo efficient photoredox upon exposure to room light; freshly prepared solutions were kept in darkness.
(25) Guenther, P. R.; Linck, R. G. *J. Am. Chem. Soc.* **1969**, *91*, 3769.
(26) Baxendale, J. H.; Bevan, P. L. T.; Stott, D. A. *Trans. Faraday Soc.* **1968**, *64*, 2398.
(27) Matheson, M. S.; Dorfman, L. M. *Pulse Radiolysis*; MIT Press: Cambridge, MA, 1969.
(28) Kitson, R. E. *Anal. Chem.* **1950**, *22*, 664.

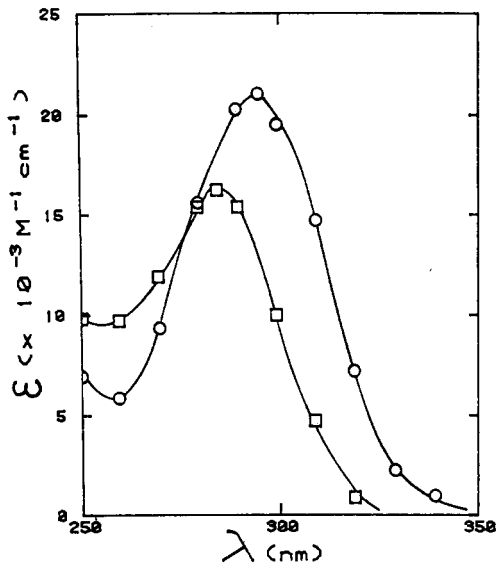

Figure 1. Transient absorption spectra measured 60 μs after the pulse irradiation of N_2O-saturated solutions containing 52 μM PNPA and 0.1 M 2-propanol at pH 7.2 (○) and pH 0.7 (□). The spectra are corrected for loss of the substrate.

the primary radicals react with the latter, to produce the reducing radicals in the presence of the Co(III) complex.

Results

Formation and Spectra of Transients. Transient absorption spectra were determined at pH 7 in pulse-irradiated N_2O-saturated solutions containing 45–55 μM complex, 0.5 mM phosphate buffer, and either 0.1 M 2-propanol or 0.1 M formate; acidic solutions contained similar concentrations of the complex, 0.1 M 2-propanol, and 0.1–1.0 M $HClO_4$. Under these conditions, the secondary reducing radicals are formed in less than 50 ns. Absorbance measurements were taken at the completion of the reaction of the reducing radicals, $^{\bullet}C(CH_3)_2OH$ or $^{\bullet}CO_2^-$, with each complex 50–100 μs after the pulse. The transient spectra obtained were independent of the identity of the precursor reducing radical. The growth of the transient absorbance is accompanied by bleaching of the parent complex absorbance; the observed transient spectra were corrected for the bleaching by using the UV–visible spectra of unpulsed samples of each complex solution and relevant dosimetry data. The corrected transient spectra obtained in neutral and acidic solution from the interaction of $^{\bullet}C(CH_3)_2OH$ with the PNPA complex are shown in Figure 1. Corrected spectral maxima for the transients formed from the Co(III) complexes are shown in Table II for neutral and acidic solutions. Molar absorbances at the maxima of the major bands are typically 1–3 × 10^4 M^{-1} cm^{-1}.

Compared with the results in neutral solution, the transient spectra in acidic solution characteristically have peak maxima that are blue-shifted by <10 nm with 10–15% lower molar absorbances; proportionately greater absorbance in the visible region relative to the UV region is also evident. Absorbance near the peak maxima was monitored as a function of pH for the phenylacetato series (ONPA, MNPA, PNPA, DNPA) leading to typical "titration curves", from which pK_a values of the intermediates of ~2.8 were evaluated. These pK_a values are similar to those obtained previously for the intermediates of the nitrobenzoato complex series[17] and for the free nitrobenzoate radicals.[18]

For both the phenylacetato and the cinnamato (ONCM, MNCM, PNCM) series, the transient spectra of the complex intermediates at pH 7 were compared with those of the analogous free ligand radicals. N_2O-saturated solutions containing 50 μM complex or free ligand and 0.1 M formate were pulsed, and absorbance measurements were taken after 100 μs. With one exception, the wavelength positions and molar absorbances of the peak maxima were the same within experimental error for the transients of the free ligands and the complexes. For the *p*-nitrocinnamato analogues, the spectral peak of the complex

Table II. Spectral Maxima and Rate Constants of Formation of One-Electron-Reduced Transient Species

	pH 7			pH 0–1	
complex	λ_{max},[d] nm	$k(^{\bullet}R)$[a-c]	$k(^{\bullet}CO_2^-)$[a,b]	λ_{max},[d] nm	$k(^{\bullet}R)$[a-c]
ONBZ		2.0	2.0	280	
MNBZ	290	2.5	1.5	280	
PNBZ	330	~4	1.9	310	
ONPA	290	2.6	1.3	*280*, 420	1.3
MNPA	290	1.9	1.5	<*280*, 440	2.3
PNPA	300	1.7	1.4	<*280*, 440	1.7
DNPA	295		3.9	290	2.5
OMCM	*300*, 380	2.0	1.9	290, *370*	1.5
MNCM	300	2.0	1.2	*290*, 350	3.0
PNCM	*310*, 370	3.9	1.4	300, *350*	2.6
PNPB	*300*, 400	2.2			
PNGB	330	3.5		310	
PNDG	325	2.8		300	2.6
PNNC	320	2.8			
PNNS	325	2.7			
PNOS	300	1.8			
PNPO	<300	2.9			
NCYC	380	2.0			

[a] ±10% error. [b] In units of 10^9 M^{-1} s^{-1}. [c] $^{\bullet}R$ = $^{\bullet}C(CH_3)_2OH$. [d] Major peak in italics.

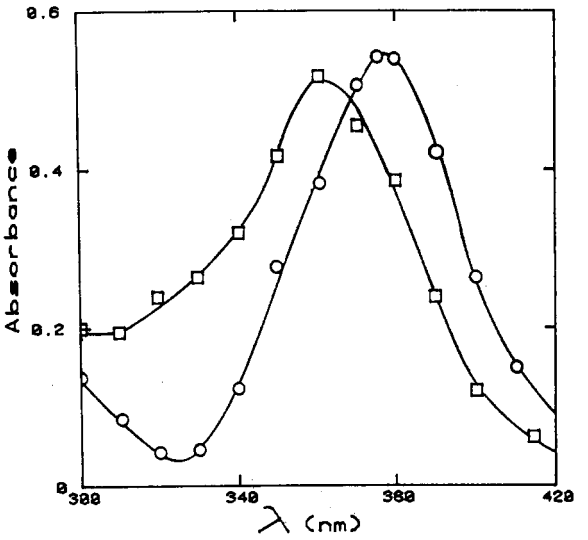

Figure 2. Transient absorption spectra measured 100 μs after the pulse irradiation of N_2O-saturated solutions containing 0.1 M formate and either 50 μM PNCM (○) or free *p*-nitrocinnamate (□) at pH 7. The spectra are corrected for the loss of the substrate.

transient was red-shifted by 15 nm compared with that of the free ligand radical, as shown in Figure 2.

Also included in Table II are the rate constants for the reactions of $^{\bullet}C(CH_3)_2OH$ and $^{\bullet}CO_2^-$ with each substrate complex, determined from the pseudo-first-order kinetics of the formation of the transient absorptions for [complex] = 20–100 μM. With few exceptions, these rate constants are uniformly 1–3 × 10^9 M^{-1} s^{-1} regardless of the identity of the precursor radical. The reaction of $^{\bullet}C(CH_3)_2OH$ with the PNPO complex forms the reduced product in two stages (*vide infra*); the rate constant of the faster formation is shown in Table II.

Transient Decay. The decay of the transient intermediates are dependent on the nature of the nitro ligands, the pH, and the ionic strength of the solution medium. At pH 7, the intermediates from all the complexes studied, with exceptions as noted, decay by a single first-order process with values of k_I that are independent of [complex] (15–100 μM), radiation dose (3–21 Gy), and the wavelength of observation. In Table III are shown the values of k_I at ~25 °C for the intermediates obtained from both $^{\bullet}C(CH_3)_2OH$ and $^{\bullet}CO_2^-$; values of k_I in 2-propanol solutions are up to 3 times larger than those in formate solutions. The effect of ionic medium was confirmed in 2-propanol solutions at pH 7 containing 0.33 M Na_2SO_4, where a similar trend toward de-

Table III. Rate Constants and Activation Parameters for Intramolecular Electron Transfer at pH 7[a]

complex	k_I,[b] s^{-1}	k_I,[c] s^{-1}	k_I,[d] s^{-1}	$\Delta H^{\ddagger}$,[c] kcal mol^{-1}	$\Delta S^{\ddagger}$,[c] cal mol^{-1} K^{-1}
ONBZ	4.0×10^5	8×10^4		~4	−24
MNBZ	1.5×10^2	1.9×10^2		17	+8
PNBZ	2.6×10^3	2.8×10^3		17	+14
ONPA	3.5×10^4	6.1×10^4	7.0×10^4	7	−14
MNPA	1.0×10^2	1.8×10^2	4.2×10	18	+11
PNPA	3.9×10^2	6.0×10^2	1.3×10^2	16	+7
DNPA	8.0×10^3	1.3×10^4			
ONCM	1.7×10^3	1.6×10^3	6.7×10^2	11	−8
MNCM	3.1	6.4	4.0	6	−35
PNCM	4.8×10^2	5.8×10^2	1.8×10^2	18	+14
PNPB	1.5×10^2	3.2×10^2	7.8×10	13	−4
PNGB	5.8	1.9×10	1.0×10	7	−29
PNDG	1.5×10^3	2.6×10^3	7.4×10^2	14	+3
PNNC		1.0×10^3		8	−20
PNNS		6.8×10^3		16	+12
PNOS		$<10^2$			
PNPO		1×10^3		4	−30
NCYC		1×10^3		8	−18

[a] ±10% error in k_I; ±20% error in $\Delta H^{\ddagger}$ and $\Delta S^{\ddagger}$. [b] In 0.1 M formate. [c] In 0.1 M 2-propanol. [d] In 0.1 M 2-propanol and 0.33 M Na_2SO_4.

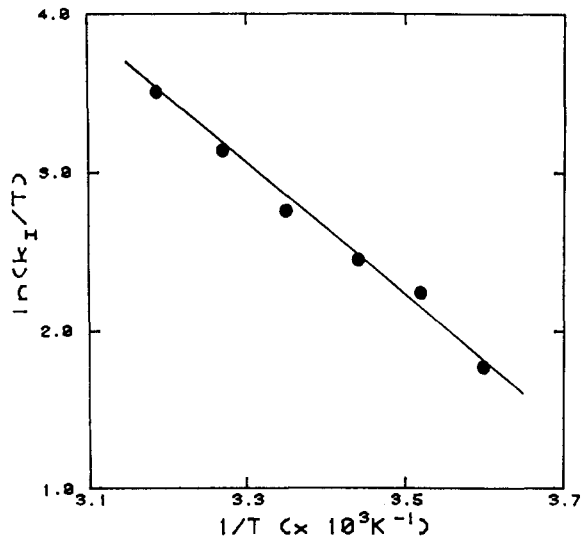

Figure 3. Plot of ln (k_I/T) vs. $1/T$ for the transient intermediate generated in the pulse irradiation of N_2O-saturated solutions containing 50 μM PNCM and 0.1 M 2-propanol at pH 7.

creased rate with increased ionic strength is observed.

The values of k_I were examined as a function of temperature over the range 5–45 °C in 2-propanol solutions at pH 7. From the linear Eyring plots of the rate data (ln k_I/T vs. $1/T$), estimates of the activation parameters, $\Delta H^{\ddagger}$ and $\Delta S^{\ddagger}$, were made from the slope ($=-\Delta H^{\ddagger}/R$) and intercept ($=\ln(k/h) + \Delta S^{\ddagger}/R$);[29] a plot of the rate data for the PNCM complex is shown in Figure 3. The activation data thus obtained are included in Table III. A very broad variation in the activation parameters is observed, with values of $\Delta H^{\ddagger}$ and $\Delta S^{\ddagger}$ ranging from 6 to 18 kcal mol^{-1} and −35 to +14 cal mol^{-1} K^{-1}, respectively.

Some experimental complexity was observed for two complexes. For NCYC, the decay of the transient intermediate at 300 and 400 nm follows neither simple first- nor second-order kinetics. From a computerized kinetic data analysis, the overall decay process is best fitted as a mixed first- and second-order reaction, in which the second-order component dominates the first two half-lives of the reaction when the [transient] is greatest. The initial rate of absorbance change depends on both the dose and wavlength of observation, consistent with the second-order character of the dominant process in the earliest stages of the reaction. Analysis of the decay for the third half-life and beyond as first-order generates a rate constant that is independent of wavelength, dose and [NCYC]. This rate constant is taken as k_I and is comparable to those shown for the other complexes in Table III. When monitored as a function of temperature, this first-order component of the overall decay exhibits the activation parameters included in Table III; the accuracy of these data is, of course, less than that of the other entries in the table. The final spectrum of an irradiated solution of the NCYC complex shows the formation of the Co(II)–NCYC product, as characterized by absorbance growth at 340 nm and an isosbestic point at 290 nm.

The reaction of $^{\bullet}C(CH_3)_2OH$ with PNPO at pH 7 is dominated spectrally by an absorbance growth at ~400 nm, characteristic of the free ligand, in two stages. The first stage, which is complete within ~100 μs, accounts for 60% of the total absorbance growth and is pseudo first order in [PNPO]; this process is interpreted as the direct interaction of the $^{\bullet}C(CH_3)_2OH$ radical with the Co(III) center. In addition, a transient absorbance having λ_{max} < 300 nm is produced in this initial timeframe; at $\lambda > 300$ nm, this transient absorbance is overwhelmed by the bleaching of the parent complex. The slower process, which is complete within ~2 ms, is characterized by the simultaneous loss of absorbance at ~300 nm and growth at ~400 nm. This process is first order, independent of [PNPO] and radiation dose at 300 and 400 nm. The value of k_I and the activation parameters for the slower process are included in Table III.

With three exceptions, the decays of the initial transients in 1 M $HClO_4$ solutions containing 0.1 M 2-propanol exhibit second-order kinetics, with dependences of the initial rate of absorbance decay on dose and wavelength. The second-order rate constants, $2k_{II}$, were determined from the transient decay data at the spectral peak maximum of each complex and are shown in Table IV. The ONBZ, ONPA, and DNPA complexes decay via first-order kinetics with rate constants that are independent of [complex] (Table IV).

Table IV. Kinetic and Yield Data in Acidic and Neutral Solutions[a]

complex	$2k_{II} \times 10^{-8}$,[b,c] M^{-1} s^{-1}	G_{Co}[d]	G_{Co}[c]	k_I,[c] s^{-1}
ONBZ	[e]	6.2	6.2	5.8×10^3
MNBZ	1.0	5.4	<0.6	<0.3
PNBZ	1.5	6.2	4.8	5
ONPA	[e]	6.4	4.9	1.6×10^3
MNPA	1.3	6.4	0.5	1
PNPA	1.1	5.9	0.6	1
DNPA	[e]			2.1×10^3
ONCM	2.1	6.5	4.9	2×10
MNCM	6.1	6.5	0.5	2
PNCM	3.6	6.5	6.1	1×10^2
PNPB	4.8	6.5	1.6	6
PNGB	2.9	6.3	0.4	1
PNDG	0.7	6.4	6.1	6×10

[a] ±10% error in $2k_{II}$ and G_{Co}. [b] Determined at λ_{max} of transient intermediate. [c] pH ~0. [d] pH ~7. [e] First-order decay; k_I measured directly.

Yields of Co^{2+}. G values for the formation of Co_{aq}^{2+} (G_{Co}) were determined in γ-irradiated N_2O-saturated solutions containing 0.1 M 2-propanol and 5×10^{-4} M complex at pH 7 and pH 0; these yields are shown in Table IV. Within experimental error, Co_{aq}^{2+} is generated quantitatively in neutral solution in all cases. In acidic solution, the different complexes exhibit considerable variation in the yield of Co_{aq}^{2+}.

Discussion

The interaction of reducing radicals (Red) with Co(III) complexes containing nitrophenyl ligands of the form Co^{III}–Y–X–$PhNO_2$ produces coordinated ligand radicals according to reaction 2. The acidic and basic forms of the reduced intermediate are

$$Co^{III}\text{–Y–X–}PhNO_2 + Red \rightarrow Co^{III}\text{–Y–X–}PhNO_2^{\bullet -} + Ox \quad (2)$$

$$Co^{III}\text{–Y–X–}PhNO_2^{\bullet -} + H^+ \rightleftarrows Co^{III}\text{–Y–X–}PhNO_2{}^{\bullet}H \quad (3)$$

related through equilibrium reaction 3. Variations in the peak positions and molar absorbances of the coordinated nitrophenyl

(29) Frost, A. A.; Pearson, R. G. *Kinetics and Mechanism*; Wiley: New York, NY, 1961; p 99.

radicals in Table II reflect differences in the distribution of electron spin density over the aromatic ligand structure.[17,18]

For the nitrobenzoato complexes, a partitioning of the reduction by e_{aq}^- between the metal center and the coordinated nitro group was previously observed.[17] A quantitatively similar extent of reductive partitioning is observed for the reactions of e_{aq}^- with the phenylacetato series of complexes.[30] With one exception (PNPO) to be discussed later, the weaker reducing radical, $^{\bullet}C(CH_3)_2OH$, reacts only at the nitro site of the complexes; this conclusion is based on the similarity of the observed molar absorbances of the transients derived from complexed and uncoordinated nitrophenyl molecules. The partitioning of reduction of the nitro complexes by e_{aq}^- (and $^{\bullet}C(CH_3)_2OH$ with PNPO) probably reflects a kinetic competition between the reducible nitro and metal sites for the incoming radical.

Intramolecular Electron Transfer. The coordinated ligand radicals of the complexes in Table II decay by first-order kinetics at pH 7, with rate constants that are independent of the [complex] and radiation dose; for the NCYC complex transient, a second-order decay competes with the first-order process. Inasmuch as Co_{aq}^{2+} is produced quantitatively with respect to the precursor radicals at pH 7, this first-order process is assigned to the reduction of the Co(III) center by the coordinated nitrophenyl radical at a remote site on each complex, i.e. as intramolecular electron transfer. For the Co(III)–pentaammine complexes, this IET would be followed by rapid spin relaxation of the Co(II) center and ligand labilization, as shown in reactions 4 and 5. This reaction sequence

$$Co^{III}\text{–Y–X–PhNO}_2^{\bullet-} \rightarrow Co^{II}\text{–Y–X–PhNO}_2 \quad (4)$$

$$Co^{II}\text{–Y–X–PhNO}_2 \rightarrow Co_{aq}^{2+} + \text{Y–X–PhNO}_2 \quad (5)$$

has been demonstrated for the PNBZ complex, for which pulse conductometric measurements show that Co_{aq}^{2+} is generated at the same rate as loss of the transient absorbance of the coordinated ligand radical.[31] In the case of the tetraaza macrocyclic NCYC complex where the low spin configuration of Co(II) is stabilized,[32] there would be no spin relaxation and ligand labilization. The values of k_I shown in Table III are taken as rate constants of IET for the complexes, where the donor nitro radical is separated from the Co(III) acceptor by bridging groups having variable flexibility and π-conjugation characteristics and by variable lead-in groups.

The nitrophenyl carboxylato complexes in Table III have the same donor, lead-in, and acceptor groups. Inasmuch as the E° values for the $PhNO_2/PhNO_2^{\bullet-}$ couple vary little with the isomeric disposition of the nitro group on the ring,[18] E° for the IET is also expected to vary little for this series of complexes. Specifically, with $E^\circ(A_5Co^{III}L/A_5Co^{II}L) \sim 0.1$ V[14] and $E^\circ(PhNO_2/PhNO_2^{\bullet-})$ between –0.3 and –0.4 V,[18] the driving force for IET is ~0.4–0.5 V. This favorable driving force is significantly greater than that exhibited in binuclear Co^{III}–Ru^{II} systems, which have negative driving forces and are driven by the irreversibility of the rapid ligand labilization of the Co(II) product complex.[14] The near constancy of the E° values for the IET within the complexes suggests that the observed 10^4-fold variation in the values of k_I derives from intrinsic kinetic factors, rather than from a thermodynamic basis. That intrinsic structural features of the varied bridging groups provide the dominant controlling influence on the rates of IET is supported by the activation data included in Table III. The striking variation in these parameters indicates that several mechanisms of IET operate in this series of complexes, which depend on the structural nature of the bridge.

If one assumes that the nitro radical has a molecular geometry similar to that of the parent nitrophenyl moiety, structural features can be approximated from Ealing CPK space-filling molecular models.[33] Four different mechanisms are derived in this way. The first of these is designated as "resonance-assisted through-chain" IET, which operates in the PNBZ and PNCM complexes and is characterized by large positive values of $\Delta H^{\ddagger}$ and moderately positive values of $\Delta S^{\ddagger}$. From a structural perspective, there is no configuration available in these complexes that brings the donor and acceptor sites into a close proximity to allow overlap of the electronic orbitals of the reactive sites. However, delocalized π-conjugation is possible that extends from the nitro radical to the carboxyl lead-in group. For these complexes, the π-bridge is proposed to mediate the transfer of an electron. The values of $\Delta H^{\ddagger}$ probably reflect barriers associated with a substantial Franck–Condon requirement for the uncoupled donor–acceptor centers and an orbital symmetry mismatch between the carboxyl lead-in group and the Co(III) center; the symmetry barrier has been previously noted for IET in the nitrobenzoato complexes.[17] The positive values of $\Delta S^{\ddagger}$ can be rationalized on the basis of the charge distribution and dielectric environment in the activated complex, which is intermediate between separated $(Co^{III}O_2C–)^{2+}$ and $–NO_2^{\bullet-}$ centers in the precursor complex and separated $(Co^{II}O_2C–)^{+}$ and $–NO_2$ centers in the successor complex. Structure breaking in the polar solvent medium would likely accompany the diminished charge density during activation, resulting in positive values of $\Delta S^{\ddagger}$; the concept of charge redistribution has been invoked for IET in binuclear Co^{III}–L–Fe^{II} systems.[34] This mode of IET through the π-bridge is analgous to the "resonance mechanism" proposed for the binuclear complexes having uninterrupted conjugation within the bridging molecule,[15] for which a red shift in the UV–visible spectral band of the Co^{III}–L entity occurs upon complexation to Fe^{II}. This spectral feature is observed for the PNCM system for which there is a 15-nm red shift in the peak maximum of the complexed nitro radical compared with that of the analogous uncomplexed radical, as shown in Figure 2.

If a configuration for the coordinated ligand radical exists that allows direct orbital overlap of the donor and acceptor sites, "direct donor–acceptor orbital overlap" IET is proposed to occur (ONBZ and ONPA) where $\Delta H^{\ddagger}$ is rather low and $\Delta S^{\ddagger}$ is moderately negative. Favorable orbital overlap provides strong vibrational coupling between the redox sites, thereby lowering the Franck–Condon barrier for IET and lowering $\Delta H^{\ddagger}$ accordingly, compared with the cases of the uncoupled PNBZ and PNCM analogues. Furthermore, the greatly reduced configurational flexibility that must accompany activation is reflected in negative $\Delta S^{\ddagger}$ values. This mechanism of IET is analogous to that proposed as "ligand bypass" for IET in binuclear complexes.[15] The ONCM system has activation parameters that are midway between those characteristic of the "resonance-assisted" and the "direct-overlap" pathways, which can both operate within this complex. The mode of IET for the ONCM complex is thus tentatively proposed as a composite of both types of mechanism, proceeding simultaneously at comparable rates.

Another type of orbital overlap mechanism is proposed for IET in the PNPB and PNDG complexes, which have moderately positive values of $\Delta H^{\ddagger}$ and near-zero values of $\Delta S^{\ddagger}$. Because of the considerable flexibility of the bridging group in these complexes, a common configuration is attainable of nearly vertical overlap of carboxyl orbitals with the aromatic carbon atom disposed para to the nitro radical. It is known that the spin density of the ligand radical is not fully localized on the nitro group but is partially dispersed over the ring structure, with 15% residing on the para carbon atom.[18] Such "indirect overlap" provides a means of channeling spin density into the lead-in group of the acceptor site, thereby facilitating IET. Again, the bridge does not mediate the IET but provides a configuration for partial "ligand bypass". The values of $\Delta H^{\ddagger}$ reflect a significant Franck–Condon barrier that arises from poor coupling between the donor and acceptor sites. Two opposing effects may account for the near-zero values of $\Delta S^{\ddagger}$. On the one hand, the severe

(30) The fraction of initial reduction of the Co^{III} center by e_{aq}^- for the MNPA, PNPA, and DNPA complexes is 0.47, 0.26, and 0.35, respectively. The procedure for determining these fractions is presented in ref 17.
(31) Simic, M.; Lilie, J. *J. Am. Chem. Soc.* **1974**, *96*, 291.
(32) Rillema, D. P.; Endicott, J. F.; Kane-Maguire, N. A. P. *J. Chem. Soc., Chem. Commun.* **1972**, 495.
(33) Hoffman, M. Z.; Whitburn, K. D. *J. Chem. Educ.* **1981**, *58*, 119.
(34) Szecsy, A. P.; Haim, A. *J. Am. Chem. Soc.* **1982**, *104*, 3063.

restriction of flexibility of the bridge into a specific configuration for activation reduces $\Delta S^{\ddagger}$. On the other hand, the lower charge concentration in the dielectric medium as the $(Co^{III}O_2C-)^{2+}$ region comes in close proximity to the $-NO_2^{\bullet-}$ group during activation increases $\Delta S^{\ddagger}$. Apparently, these opposing factors on the activation entropy nearly cancel each other for these complexes.

The values of k_I and the activation parameters for the PNPA complex suggest that the mode of IET in this case may be a composite of the "resonance-assisted" and "indirect-overlap" mechanisms. Although the $-CH_2-$ group breaks the π-conjugation in the bridging ligand, it is estimated from ESR measurements on the uncoordinated (*p*-nitrophenyl)acetate radical that the carbon atom of this group bears ~10% of the total spin density of the unpaired electron.[35] Such a minor delocalization into the lead-in group in the complex may be sufficient for a component of the "resonance" mechanism to operate simultaneously with an "indirect-overlap" pathway.

A fourth type of mechanism of IET is proposed for MNCN, PNGB, and PNPO, all of which have low values of $\Delta H^{\ddagger}$ and large negative values of $\Delta S^{\ddagger}$. For each of these complexes, there is no extended π-conjugation between the redox sites and there are no configurations of the bridging group that allow "direct" or "indirect" orbital overlap of the donor and acceptor/lead-in orbitals, so that there is no coupling between the nitro radical and the metal center to assist "bypass" transfer. Very small coupling between donor and acceptor sites is a primary condition for nonadiabatic electron transfer, which is characterized by large negative values of $\Delta S^{\ddagger}$ and derives from a low transfer probability in the activated state of the process.[36] The value of k_I for the PNPO complex is substantially larger than that for the MNCM and PNGB complexes, which may reflect the 2–3 kcal mol^{-1} reduction in the value of $\Delta H^{\ddagger}$ for this system.

We must point out that the activation data for the MNPA and MNBZ complexes do not correlate with any of the mechanisms for IET already proposed for the other complexes. Modes of IET in these systems may be composites of the proposed mechanisms or may be separate undetermined pathways.

Variable Lead-In Groups. PNNC, PNNS, PNOS, PNPO, and NCYC represent *p*-nitro complexes having different lead-in groups to the Co(III) center. Although the values of k_I for these complexes vary little with the nature of the lead-in group, considerable variation occurs in $\Delta H^{\ddagger}$ and $\Delta S^{\ddagger}$ for this series, indicating that different mechanisms of IET are in operation. The activation parameters for the PNNS complex are similar to those of the PNBZ and PNCM complexes, consistent with the "resonance-assisted" mechanism of IET. A resonance structure can be drawn for the PNNS complex that consitutes a conjugated π-bridge from the donor nitro group to the Co(III) acceptor center. However, the PNOS complex, which has an isoelectronic $-OSO_2-$ lead-in group, has a greatly diminished rate of IET compared with that of the PNNS complex. Although a change of mechanism may be involved, this observation may simply reflect a change in the driving force of the Co(III)/Co(II) couple with a change in the atom ligated to the metal center. Also, it is notable that the PNNC complex, having a π-bonded cyano bridge/lead-in group, does not exhibit activation parameters characteristic of the "resonance" mechanism. The activation data for this complex are more consistent with "nonadiabatic" IET, characterized by a large negative $\Delta S^{\ddagger}$ and moderately low $\Delta H^{\ddagger}$. The mechanism of the IET for the PNPO system, which has the simplest bridge/lead-in structure of all the complexes studied, namely a single O atom, was proposed earlier as "nonadiabatic". For the macrocyclic NCYC complex, the activation data also suggest that the "nonadiabatic" mechanism may operate. Overall, the mechanism of IET correlates poorly with the nature of the lead-in group in this series of complexes.

Effects of Solution Medium. Table III shows that regardless of the various mechanisms of IET proposed for the complexes, there is a general small decrease in the values of k_I with increasing ionic strength. This trend is consistent with the requirement for an "intermolecular" electrostatic interaction between the separated redox sites on the same molecule during activation. In this way, the ionic medium may affect uniformly a minor electrostatic work term associated with the activation of the separated charged donor and acceptor sites to an optimal coulombic interaction for IET. Alternatively, the effect of ionic strength may result from uniform changes in the polarization of the aqueous medium with increasing ionic concentration as reflected by a solvent reorganization barrier associated with the activation process.

As seen in Table IV, the transient intermediates of most of the nitrophenyl complexes decay by second-order kinetics in acidic solution, indicating bimolecular radical decay, probably disproportionation,[17] as represented in reaction 6. The less-than-quantitative yields of Co^{2+} in γ-irradiated acidic solutions reflect a competition between this second-order decay and the first-order IET process in reaction 7.

$$2Co^{III}\text{-Y-X-}NO_2{}^{\bullet}H \rightarrow Co^{III}\text{-Y-X-}NO_2 + Co^{III}\text{-Y-X-NO} + H_2O \quad (6)$$

$$Co^{III}\text{-Y-X-}NO_2{}^{\bullet}H \rightarrow Co^{II}\text{-Y-X-}NO_2 + H^+ \quad (7)$$

Just as the IET and bimolecular decay of the nitro radical of the NCYC complex proceed simultaneously under pulse conditions at pH 7, reactions 6 and 7 occur together for the complexed nitrophenyl radicals in γ-irradiated acidic solutions. This congruence in the rates of the first- and second-order processes probably results from two influences. First, the value of k_I is greatly diminished because of the lower driving force of the protonated nitro radicals compared with that of the unprotonated analogues of pH 7.[18] Second, it is known that protonation of uncoordinated nitrobenzoate radicals increases the rate constants of bimolecular decay by 2–3 orders of magnitude.[18] For the ONBZ, ONPA, and DNPA systems, the value of k_I is sufficiently large in acidic solution to override any competition by reaction 5, so that quantitative yields of Co_{aq}^{2+} are obtained.

Values of k_I ($=k_7$) for the other complexes in acidic solution can be estimated from the experimental values of G_{Co}, $2k_{II}$ ($=2k_6$), and the radiation dose rate (D_r) through an application of the steady-state approximation for the radiation-generated reducing radicals and the protonated ligand radical coordinated to Co(III) ($CoL^{\bullet}H$) in reactions 1–3, 6, and 7. The rate of formation of $^{\bullet}R$ is equal to $G_R D_r$, where $G_R = G_e + G_{OH} + G_H$; $[R^{\bullet}] = G_R D_r / k_2[CoL]$, where CoL is the Co(III) substrate, and $[CoL^{\bullet}H] = (-k_I + [k_I^2 + 8k_{II}G_R D_r]^{1/2})/4k_{II}$. Now, G_{Co} will be less than G_R as a result of the competition between reactions 6 and 7; $G_{Co} = G_R[k_I/(k_I + 2k_{II}[CoL^{\bullet}H])]$. Substituting for $[CoL^{\bullet}H]$ in the latter expression and rearranging results in expression 8; the values of k_I thus calculated, from $D_r = 1.1 \times 10^2$ Gy min^{-1} and $G_R = 0.62$ μM Gy^{-1}, are given in Table IV.

$$k_I = \left[\frac{8k_{II}G_R D_r}{[(2G_R/G_{Co}) - 1]^2 - 1} \right]^{1/2} \quad (8)$$

These estimated values of k_I for solutions 1 M in $HClO_4$ can be compared with the measured values of k_I at pH 7 at 1 M ionic strength. In such a comparison, it is apparent that the kinetic effect of the isomeric position of the nitro group on the aromatic moiety of a complex series having a particular type of bridge is similar in acid and neutral solution, i.e. for the protonated and deprotonated forms of the coordinated nitro radicals. Specifically, the meta isomers of the benzoato, phenylacetato, and cinnamato series have significantly slower rates of IET than do the ortho and para analogues. The effect of isomeric position of the nitro group on k_I has been previously explained for the benzoato complexes at pH 7 as arising as a result of the electron spin density distribution of the nitro radical over the aromatic ring.[17] Thus, protonation of the nitro group lowers the total spin density on the ring[18,37] but does not significantly change the distribution of the spin density. The greatest kinetic effect of nitro protonation might

(35) Neta, P., unpublished observation; $a^H = 2.59$.
(36) Taube, H. *Adv. Chem. Ser.* **1977**, *No. 162*, 127.
(37) Cohen, H.; Meyerstein, D. *J. Chem. Soc., Dalton Trans.* **1975**, 2477.

be expected for the direct and indirect "bypass" mechanisms of IET, inasmuch as assistance in maintaining the specific configuration for maximal orbital overlap may be obtained from H-bonding interactions between the nitro group and the coordinated ammine ligands. However, the diminished rates in acid solution for the complexes exhibiting these modes of IET (ONBZ, ONPA, PNPB, PNDG) are not significantly different from those of the other complexes in the series, suggesting that a requirment for H-bonding in these "bypass" mechanisms may be of minor importance.

When compared with values of k_I obtained at pH 7 at an ionic strength of 1 M, the values of k_I in acidic solution are uniformly ~50 times slower for the ortho, meta, and para isomers of the phenylacetato complexes, although different mechanisms of IET operate in neutral solution for each complex in this series. For the PNBP, PNGB, and PNDG complexes, which also exhibit different pathways of IET, nitro protonation uniformly decreases the values of k_I by ~15 times. However, no such uniform reduction in rate occurs for the cinnamato series. The general uniformity in the decreases in the values of k_I suggests that protonation of the nitro radical affects only the driving force for the IET, while leaving the mechanism unaffected in most cases.

Acknowledgment. The use of the pulse radiolysis facilities at the U.S. Army Natick Research and Development Center and CFKR is gratefully acknowledged. CFKR is supported jointly by the Biomedical Research Technology Program of the Division of Research Resources of NIH (Grant RR 00886) and by The University of Texas.

Registry No. ONBZ, 62714-55-0; MNBZ, 62714-56-1; PNBZ, 36445-08-6; ONPA, 103241-52-7; MNPA, 103241-53-8; PNPA, 40544-48-7; DNPA, 103241-54-9; ONCM, 103241-55-0; MNCM, 103241-56-1; PNCM, 103241-57-2; PNPB, 103241-58-3; PNGB, 103241-59-4; PNDG, 103241-60-7; PNNC, 68033-17-0; PNNS, 78891-44-8; PNOS, 76024-72-1; PNPO, 80679-83-0; NCYC, 103258-82-8; $NaHCO_3$, 141-53-7; $^{\bullet}CO_2^-$, 14485-07-5; $^{\bullet}C(CH_3)_2OH$, 5131-95-3; 2-propanol, 67-63-0.

Contribution from the Laboratory of Chemistry, Kagawa Nutrition College, Sakado, Saitama 350-02, Japan, and Department of Chemistry, Faculty of Science, Nagoya University, Chikusa-ku, Nagoya 464, Japan

Micellar Effects on the Kinetics of the Aquation and the Base Hydrolysis of Tris(1,10-phenanthroline)iron(II) and Chloropentaamminecobalt(III) Ions

Satoshi Tachiyashiki*[1a] and Hideo Yamatera[1b]

Received October 16, 1985

Kinetics of the aquation and the base hydrolysis of $Fe(phen)_3^{2+}$ and $CoCl(NH_3)_5^{2+}$ were studied in aqueous SDS solutions at 35.0 °C. The rate constant of the aquation of $Fe(phen)_3^{2+}$ increased from 4.4×10^{-4} to 6.6×10^{-4} s^{-1} with an increase in the SDS concentration below the critical micelle concentration (cmc), while that of the base hydrolysis decreased from 0.085 to 0.010 mol^{-1} dm^3 s^{-1}. The rate constants showed no remarkable changes above the cmc. The rate constants of the aquation and the base hydrolysis of $CoCl(NH_3)_5^{2+}$ changed only above the cmc (from 6.1×10^{-6} to 8.1×10^{-6} s^{-1} and from 3.4 to 0.039 mol^{-1} dm^3 s^{-1}, respectively). The changes in the rate constants of the $Fe(phen)_3^{2+}$ reactions below the cmc were related to the formation of premicellar aggregates of the complex ion and the monomeric dodecyl sulfate ions through hydrophobic interaction, while the changes in the rate constants of the $CoCl(NH_3)_5^{2+}$ reactions above the cmc were explained by a partition of the complex ions to a micellar phase through electrostatic interaction. Effects of added NaCl on the rate behavior of the complexes in the micellar solutions were discussed by using an ion-exchange model. The role of the hydrophobic effect on the premicellar and micellar catalyses of the reaction is also discussed.

Introduction

The effects of micellar systems on chemical reactions have been studied extensively especially for organic reactions.[2,3] On the other hand, relatively few works have been carried out for inorganic reactions. So far, studies were made on electron-transfer reactions involving metal complexes,[4-10] and complex formation of Ni^{2+} or Mn^{2+} with organic ligands.[11-14] These studies are important not only from the viewpoint of inorganic reaction mechanisms but also from biochemical aspects, i.e., as models of electron-transfer and ligand-exchange reactions on the surface of a biomembrane or at the interface of a globular protein. Among ligand-exchange reactions, the aquation and the base hydrolysis of metal complex ions have rarely been studied in surfactant solutions[15] in spite of their extensive studies in aqueous solutions.[16,17] These reactions are appropriate as models for investigating the effects of electrostatic and hydrophobic interactions on ligand-exchange reactions at interfaces.

In the course of studies of the effects of micelles on chemical reactions, catalytic effects were also observed in dilute surfactant solutions below the critical micelle concentration (cmc).[4,5,7,9,12-14,18,19] The changes in the reaction rates were attributed either to the interaction of reactants with premicellar aggregates of surfactants,[5,20] to the interaction of reactants with monomeric species of surfactants to form aggregates below the

(1) (a) Kagawa Nutrition College. (b) Nagoya University.
(2) Fendler, J. H.; Fendler, E. J. *Catalysis in Micellar and Macromolecular Systems*; Academic: New York, 1975.
(3) *Reaction Kinetics in Micelles*; Cordes, E. H., Ed.; Plenum: New York, 1973.
(4) Bruhn, H.; Holzwarth, J. *Ber. Bunsen-Ges. Phys. Chem.* **1978**, *82*, 1006-11.
(5) Bhalekar, A. A.; Engberts, J. B. F. N. *J. Am. Chem. Soc.* **1978**, *100*, 5914-20.
(6) Pelizzetti, E.; Pramauro, E. *Inorg. Chem.* **1979**, *18*, 882-3.
(7) Pelizzetti, E.; Pramauro, E. *Inorg. Chem.* **1980**, *19*, 1407-9.
(8) Ponganis, K. V.; Araujo, M. A.; Hodges, H. L. *Inorg. Chem.* **1980**, *19*, 2704-9.
(9) Pramauro, E.; Pelizzetti, E.; Diekmann, S.; Frahm, J. *Inorg. Chem.* **1982**, *21*, 2432-6.
(10) Araujo, M. A.; Hodges, H. L. *Inorg. Chem.* **1982**, *21*, 3167-72.
(11) James, A. D.; Robinson, B. H. *J. Chem. Soc., Faraday Trans. 1*, **1978**, *74*, 10-21.
(12) Holzwarth, J.; Knoche, W.; Robinson, B. H. *Ber. Bunsen-Ges. Phys. Chem.* **1978**, *82*, 1001-5.
(13) Diekmann, S.; Frahm, J. *J. Chem. Soc., Faraday Trans. 1*, **1979**, *75*, 2199-210.
(14) Reinsborough, V. C.; Robinson, B. H. *J. Chem. Soc., Faraday Trans. 1*, **1979**, *75*, 2395-405.
(15) Cho, J. R.; Morawetz, H. *J. Am. Chem. Soc.* **1972**, *94*, 375-7.
(16) Basolo, F.; Pearson, R. G. *Mechanisms of Inorganic Reactions*; 2nd ed.; Wiley: New York, 1967; pp 158-93.
(17) Iida, M.; Yamatera, H. *Bull. Chem. Soc. Jpn.* **1977**, *50*, 2935-39 and references therein.
(18) Pelizzetti, E.; Pramauro, E. *Ber. Bunsen-Ges. Phys. Chem.* **1979**, *83*, 996-1000.
(19) Bunton, C. A.; Carrasco, N.; Huang, S. K.; Paik, C. M.; Romsted, L. S. *J. Am. Chem. Soc.* **1978**, *100*, 5420-5. Shiffman, R.; Rav-Acha, Ch.; Chevion, M.; Katzhendler, J.; Sarel, S. *J. Org. Chem.* **1977**, *42*, 3279-84. Bunton, C. A.; Romsted, L. S.; Smith, H. J. *Ibid.* **1978**, *43*, 4299-303.
(20) Okahata, Y.; Ando, R.; Kunitake, T. *J. Am. Chem. Soc.* **1977**, *99*, 3067-72.

0020-1669/86/1325-3043$01.50/0